

Hot plasma in clusters of galaxies, the largest objects in the universe

Craig L. Sarazin

Department of Astronomy, University of Virginia,
530 McCormick Road, Charlottesville, VA 22903-0818

(Dated: November 2, 2018)

Clusters of galaxies are the largest organized structures in the Universe. They are important cosmological probes, since they are large enough to contain a fair sample of the materials in the Universe, but small enough to have achieved dynamical equilibrium. Clusters were first discovered as concentrations of hundreds of bright galaxies in a region about 3 megaparsecs (10 million light years) across. However, the dominant observed form of matter in clusters is hot, diffuse intergalactic gas. This intracluster plasma has typical temperatures of $T \sim 7 \times 10^7$ K, and typical electron densities of $n_e \sim 10^{-3}$ cm $^{-3}$. This intracluster plasma mainly emits X-rays, and typical cluster X-ray luminosities are $L_X \sim 10^{43} - 10^{45}$ erg/s. The basic properties of and physical processes in the intracluster plasma will be reviewed. Important observational constraints on plasma processes in these systems will be discussed. Recent X-ray observations of clusters of galaxies with the orbiting Chandra X-ray Observatory will be highlighted.

PACS numbers: 95.30.Qd, 98.65.Cw, 98.65.Hb

I. INTRODUCTION

Clusters of galaxies are the largest relaxed structures in the Universe. They were initially discovered in optical observations, where clusters appear as concentrations containing $\sim 10^2$ bright galaxies and $\sim 10^3$ faint galaxies in a region which is typically ~ 2 Mpc in radius (1 megaparsec = 3.09×10^{24} cm) [1]. For example, Figure (1, left panel) shows the optical image of the central region of the nearby Coma cluster showing many galaxies. In their central regions, clusters are about 10^3 times denser than the average of material in the Universe. Clusters of galaxies are very important cosmological probes [2]. Essentially, they are the only objects in the Universe are both small enough to have achieved dynamical equilibrium during the age of the Universe, and large enough to contain a fair sample of the material in the Universe (e.g., the average ratio of baryonic to dark matter).

Although they were first observed as collections of galaxies, the dominant form of matter which has been observed in clusters of galaxies is hot diffuse plasma [3]. This intracluster medium (ICM) has typical temperatures of $\sim 7 \times 10^7$ K and typical electron number densities of $n_e \sim 10^{-3}$ cm $^{-3}$. At these temperatures, the dominant form of radiation from a plasma is X-ray emission, mainly from thermal bremsstrahlung but also from collisionally excited line emission. As a result, clusters of galaxies are generally very luminous X-ray emitters, with luminosities of $L_X \sim 10^{43} - 10^{45}$ ergs s $^{-1}$. Clusters are second only to quasars as the most luminous X-ray sources in the Universe. For example, Figure (1, right panel) shows the X-ray image of the same central region of the Coma cluster as the left panel. Although the ICM is diffuse, it fills all of the volume between and within the galaxies in clusters, and as a result its mass is large. The total mass of hot plasma in a cluster is typically $M_{\text{gas}} \sim 10^{14} M_{\odot}$, where $M_{\odot} = 1.99 \times 10^{33}$ g is the mass of the Sun. In large clusters, the total mass of hot gas exceeds the mass of all

the stars and galaxies by a factor of ~ 5 . Hot intracluster plasma is the dominant form of baryonic matter in clusters. In general, we now believe that most of the baryonic matter in the low redshift Universe is in the form of hot intergalactic plasma.

II. PHYSICAL PROPERTIES OF THE INTRACLUSTER PLASMA

The mean free paths of electrons and ions in a plasma without a magnetic field are determined by Coulomb collisions. The mean free path of electrons (which is nearly the same as that protons) is [4]

$$\lambda_e = \frac{3^{3/2}(kT)^2}{4\pi^{1/2}n_e e^4 \ln \Lambda} \approx 23 \left(\frac{T}{10^8 \text{ K}} \right)^2 \left(\frac{n_e}{10^{-3} \text{ cm}^{-3}} \right)^{-1} \text{ kpc}, \quad (1)$$

where n_e is the electron number density, the Coulomb logarithm $\ln \Lambda \approx 38$, and 1 kpc = 3.09×10^{21} cm. This is about 1% of the radius of a cluster, which suggests that the intracluster plasma can be treated as a fluid. The gyroradii in the intracluster magnetic field are much smaller than this (Sec. III).

The timescale for Coulomb collisions between electrons to bring them into kinetic equilibrium (an isotropic Maxwellian velocity distribution) is about [4]

$$t_{\text{eq}}(e, e) \approx 3.3 \times 10^5 \left(\frac{T}{10^8 \text{ K}} \right)^{3/2} \left(\frac{n_e}{10^{-3} \text{ cm}^{-3}} \right)^{-1} \text{ yr}. \quad (2)$$

The time scale for protons to equilibrate among themselves is $t_{\text{eq}}(p, p) \approx (m_p/m_e)^{1/2} t_{\text{eq}}(e, e)$ or roughly 43 times longer than the value in Equation (2). Similarly, time scale for the electrons and ions to reach equipartition (equal temperatures) is $t_{\text{eq}}(p, e) \approx (m_p/m_e)t_{\text{eq}}(e, e)$, or roughly 1870 times the value in Equation (2). All of these are shorter than the typical ages of clusters of

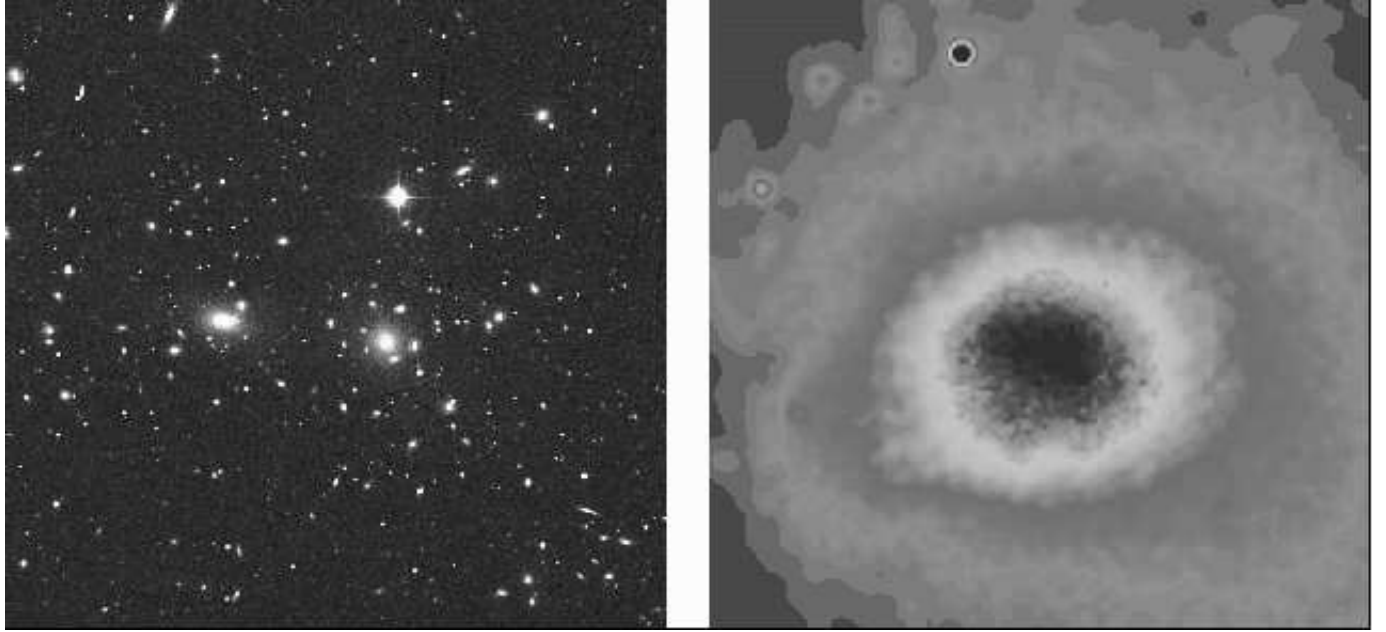


FIG. 1: The left panel shows an optical image of the central region of the nearby Coma cluster of galaxies, showing the galaxies in the cluster. The right panel shows the same region imaged in X-ray emission with the Röntgen Satellite (ROSAT). The X-ray emission comes from hot plasma at about 10^8 K which fills the volume of the cluster.

$\gtrsim 10^9$ yr. Thus, the intracluster plasma can generally be characterized by a Maxwellian distribution at a kinetic temperature T . Because the radiation field is much more diffuse than a blackbody at the kinetic temperature, the gas is far from thermodynamic equilibrium in terms of the populations of excited levels of ions and the ionization state. However, the gas is in “coronal equilibrium”; most bound electrons are in their ground levels, they are in excitation equilibrium, and the gas is in ionization equilibrium.

The sound crossing time for a cluster is

$$t_s \equiv \frac{D}{c_s} \approx 6.6 \times 10^8 \left(\frac{T}{10^8 \text{ K}} \right)^{-1/2} \left(\frac{D}{\text{Mpc}} \right) \text{ yr}, \quad (3)$$

Here, D is the diameter of the cluster, and c_s is the sound speed. This is somewhat smaller than the likely ages of clusters, so unless they are being disturbed (Sec. IV), the gas should be nearly in hydrostatic equilibrium. For a spherical cluster in hydrostatic equilibrium, the gas distribution is given by

$$\frac{1}{\rho_{\text{gas}}} \frac{dP_{\text{gas}}}{dr} = -\frac{GM(r)}{r^2}, \quad (4)$$

where $M(r)$ is the total cluster mass within a radius r . The gas pressure in the ICM is given by the ideal gas law, $P_{\text{gas}} = \rho_{\text{gas}} kT / (\mu m_H)$, where ρ_{gas} is the mass density in the gas, and μm_H gives the mean mass per particle. One often assumes that magnetic forces, pressure from relativistic particles, and other forces are relatively weak in clusters, although it is not certain that this is

correct (Sec. III). Equation (4) has been used to determine the total masses or total density profiles of clusters by solving for $M(r)$. The temperature of the ICM can be determined from observations of the X-ray spectrum of the gas, while the X-ray surface brightness can easily be de-projected to give the gas density. Such measurements indicate that the total masses of large clusters are about $10^{15} M_\odot$, which considerably exceed the total mass of all of the intracluster gas and of all the galaxies combined. As such, clusters provide some of the strongest evidence for the domination of (probably nonbaryonic) dark matter on large scales in the Universe. In a typical large cluster, $\sim 16\%$ of the mass is in hot ICM, $\sim 3\%$ of the mass is in stars and galaxies, and $\sim 81\%$ of the mass appears to be dark matter.

As is true of most materials in the Universe, the ICM consists primarily of ionized hydrogen ($\approx 71\%$ of mass) and helium ($\approx 28\%$ of mass). However, the ICM does contain a significant amount of the common heavier elements (O, Fe, etc.; $\approx 1\%$ of mass). This fraction is only about a factor of 2–3 times smaller than the fraction in the Sun. Many of these heavy elements are detected through X-ray lines observed in the spectra of clusters of galaxies; these lines occur because the heavier elements are not quite completely ionized, even at the high temperatures in clusters. Because most of the baryonic matter in clusters is in the ICM, it turns out that most of the heavy elements are actually located there as well. Hydrogen and helium are formed in the Big Bang, but the only source of the common heavier elements is fusion reactions in the centers of stars. At present, the only significant

populations of stars are located in galaxies. The dispersal of heavy element into the diffuse intracluster gas required that stars in galaxies be disrupted by supernova explosions, and that the enriched gas escape the gravity of the galaxy in which the stars are located. Detailed models for the chemical evolution of the ICM suggest that about 25% of the gas originated in stars in galaxies, and that the remaining 75% came from primordial intergalactic gas. Because there is presently about five times as much mass in the ICM as in stars and galaxies, this requires that the galaxies located in clusters lost significant amounts of their baryonic content. At present, the galactic population in clusters of galaxies consists mainly of elliptical (E) and lenticular (S0) galaxies, which have only low mass stars which do not produce a high rate of supernovae. To explain the large amounts of heavy elements in the ICM, these galaxies must have had much higher rates of star formation and supernovae at earlier times, possibly associated with the formation of the galaxies.

Initially, the very high temperature ($\sim 10^8$ K) of the ICM might seem surprising. However, this is one feature of clusters which is easily understood. Clusters of galaxies contain enormous masses of material, and have very deep gravitational potential wells. Almost any natural process which introduces gas into clusters will cause it to move very rapidly and be shock-heated to roughly the observed temperature. For example, if the ICM fell into clusters, it would be accelerated to roughly the escape speed from clusters, which is ~ 2000 km/s. A portion of the ICM may have been ejected from galaxies; galaxies in clusters move on random orbits with velocities of ~ 1000 km/s. In either case, infalling or ejected gas would encounter other gas moving at similar velocities, and would be undergo strong hydrodynamical shocks. Shocks at speeds of ~ 1000 km/s heat gas to temperatures of $\sim 10^8$ K.

III. MAGNETIC FIELDS AND RELATIVISTIC PARTICLES

Although the ICM is dominated in mass and energetically by thermal plasma, it does contain magnetic fields and populations of relativistic, nonthermal particles as well. The most direct way to measure the magnetic field in clusters of galaxies is through the Faraday rotation of the polarization of background or embedded radio sources [5]. Most strong extragalactic radio sources emit synchrotron radiation which is strongly linearly polarized. When this radiation passes through a magnetized plasma, the plane of polarization is rotated through an angle

$$\phi = (RM)\lambda^2, \quad (5)$$

where λ is the wavelength of the radiation. The rotation measure, RM , is given by

$$RM = \frac{e^3}{2\pi m_e^2 c^4} \int n_e B_{\parallel} dl, \quad (6)$$

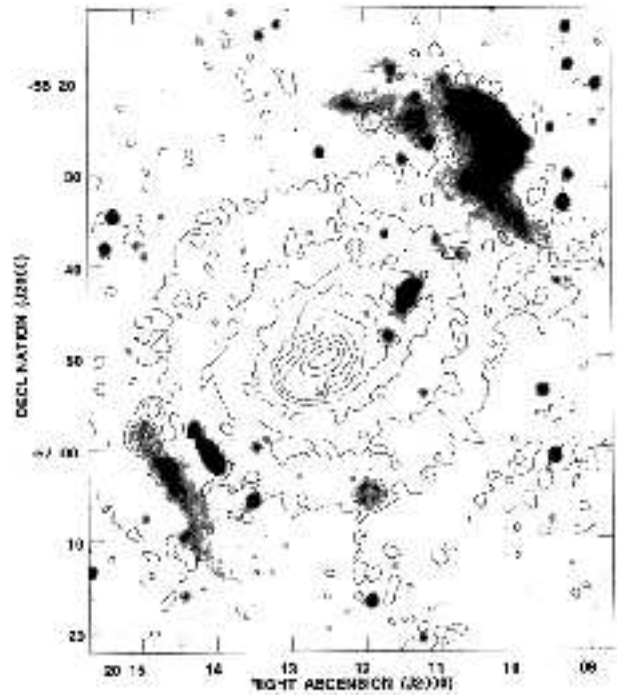


FIG. 2: The grey-scale is the radio image of the cluster Abell 3667 [7], while the contours are an X-ray image. The radio image shows two extended arcs, which are cluster radio relics, located to the southeast (lower left) and to the northwest (upper right) of the cluster center. These radio relics are believed to be associated with cluster merger shocks. (©1997, The Royal Astronomical Society.)

where l is the path length through the medium, and B_{\parallel} is the component of the magnetic field parallel to the direction of propagation of the radiation. The rotation measures seen through the central regions of clusters are $RM \sim 100$ rad m $^{-2}$. Unfortunately, Equation (6) shows that the rotation measure only determines an integral of B_{\parallel} along the line of sight, and this integral is strongly affected by the poorly known topology of the magnetic field. Field reversals along the line of sight will greatly reduce RM . If one assumes that the coherence length of the field is about 10 kpc, the rotation measure observations suggest that the typical magnetic field strength is $B \sim 5 \mu G$ [5]. This would imply that the fields are still significantly subthermal; the ratio of magnetic to gas pressures is only $(P_B/P_{\text{gas}}) \sim 0.05$. In the central regions of clusters with cooling cores (Sec. V), much larger rotations measures are observed ($RM \sim 10^4$ rad m $^{-2}$), which suggest that the magnetic fields in these regions may approach equipartition with the gas pressure.

In addition to the thermal plasma in the intracluster medium, significant population of relativistic electrons are observed in some clusters. The observations are crudely consistent with a power-law distribution for the relativistic particles; that is, $N_e(E) \propto E^{-p}$, where $N_e(E) dE$ gives the number of electrons with energies in

the range $E \rightarrow E + dE$. Similar distributions are seen in other astrophysical plasmas including the Galactic cosmic rays. However, it is likely that the particle distributions are more complex, and also vary spatially. Relativistic electrons interact with the intracluster magnetic field to produce synchrotron radio emission; the electrons which produce the emission typically have energies ~ 10 GeV. Diffuse emission, not associated with any individual galaxy, is seen in ~ 40 clusters of galaxies; when the emission is centrally located, the sources are called “cluster radio halos,” while “cluster radio relics” are peripherally located [6]. For example, Figure (2) shows two radio relic sources in the cluster Abell 3667 [7].

Relativistic electrons in clusters can also produce observable emission through the inverse Compton scattering of low energy photons; the main source of these photons in clusters of galaxies is the Cosmic Microwave Background. Typically, inverse Compton scattering produces emission which is observable either in the extreme-uv/soft X-ray band (near 0.1 keV) or in the the hard X-ray band (20–100 keV). Recently, inverse Compton hard X-ray emission has been detected from several clusters [8]. Extreme-uv/soft X-ray emission, which might also be from relativistic electrons, may have also been detected [9]. Detecting both inverse Compton and synchrotron emission from the same population of relativistic electrons is useful, because the synchrotron emission depends on the product of the energy density in relativistic electrons and that in the magnetic field, while inverse Compton emission depends on the product of the energy density in relativistic electrons and that in the Cosmic Microwave Background (which is very well determined). In principle, the combination of these two measurements allows both the total energy in relativistic electrons and the magnetic field strength to be determined. However, one needs to assume that the particles and magnetic field have the same distribution and that both are reasonably uniform, which may not be true. For the very few clusters with such data, the present observations and this simple argument suggest that the magnetic field strengths are $\sim 0.5 \mu\text{G}$, about an order of magnitude smaller than those derived from Faraday rotation. This disagreement may indicate that the assumption of a similar and uniform distribution for the particles and magnetic fields is wrong; for example, the magnetic field in clusters may be very inhomogeneous. Assuming these uncertain values are correct, the energy density and pressure in relativistic electrons may be a few percent of values for the thermal plasma in clusters. However, the total contribution from relativistic particles is also uncertain because the ions have not been detected.

IV. CLUSTER MERGERS: THE MOST ENERGETIC EVENTS SINCE THE BIG BANG

There now is considerable evidence that clusters of galaxies and other large structures in the Universe form

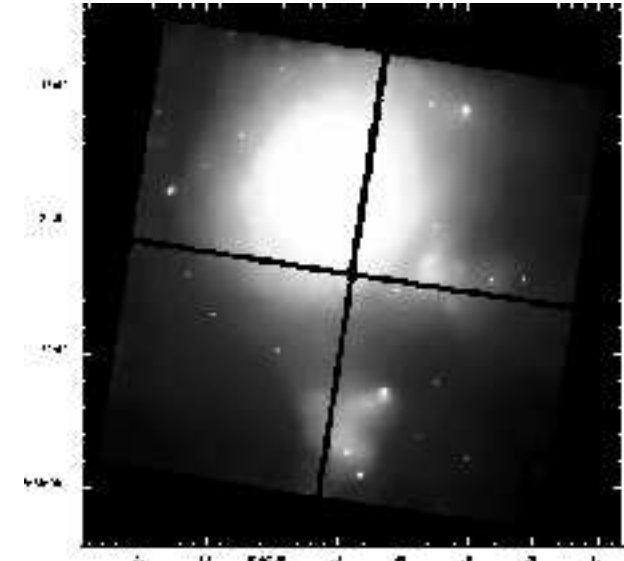


FIG. 3: The Chandra X-ray image of the merger cluster Abell 85 [11]. The grey scale burns out the central cooling flow region to show the outer parts of the cluster. Two subclusters to the south (lower middle) and southwest (lower right) are merging with the main cluster. The southwestern subcluster has a cluster radio relic. The sharp feature at the northwest of the southern subcluster is a “cold front”.

hierarchically; that is, smaller structures form first, and gravity pulls these smaller structures together to make larger structures. Clusters of galaxies form by the merger of smaller subclusters and groups of galaxies.

Major cluster mergers, in which two subclusters with a total mass of $\sim 10^{15} M_\odot$ collide together at velocities of more than 2000 km/s, are the most energetic events which have occurred in the Universe since the Big Bang itself [10]. Cluster mergers release total energies of $\sim 3 \times 10^{64}$ erg. The motions in cluster mergers are transonic, and the mergers drive shocks into the intracluster gas. In major mergers, these merger shocks dissipate total energies of $\sim 3 \times 10^{63}$ erg. Such merger shocks are, in fact, the primary heating source of the intracluster plasma. For example, Figure (3) shows the Chandra image of the merging cluster Abell 85 [11].

Hydrodynamical simulations of cluster formation and evolution have shown the importance of merger shocks [12]. The evolution of the structure of merger shocks is illustrated in Figure 4, which shows an off-center merger between two symmetric subclusters. At early stages in the merger (the first panel and earlier), the shocked region is located between the two subcluster centers and is bounded on either side by two shocks. At this time, the subcluster centers, which may contain cooling cores and central radio sources, are not affected. Later, these shocks sweep over the subcluster centers (between the first and second panels). The main merger shocks pass into the outer parts of the merging system (panel 2), and secondary shocks may appear in the inner regions (panel 3). Eventually, the cluster begins to return to equilibrium

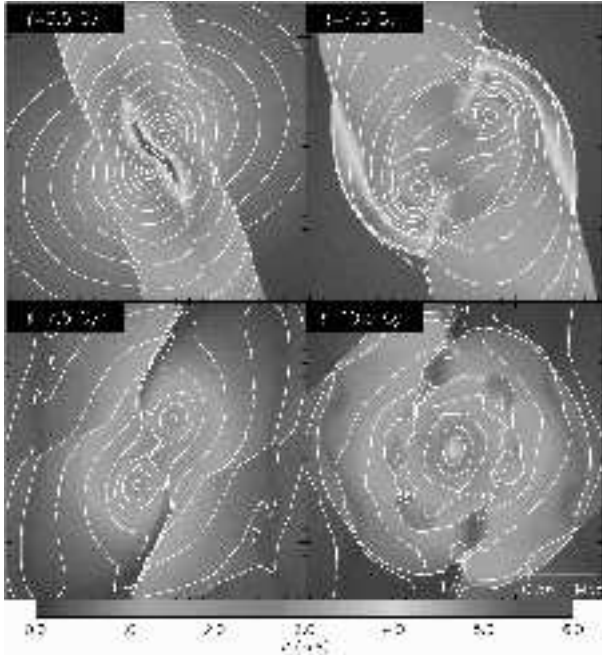


FIG. 4: The results of a hydrodynamical simulation of a symmetric, off-center cluster merger [12]. The grey scale shows the temperature, while the contours are the X-ray surface brightness. Initially, the shocked region is located between the two subcluster centers. Later, the main merger shocks propagate to the outer parts of the cluster, and other weaker shocks also occur. By the end of the simulation, the cluster is beginning to return to equilibrium.

(panel 4).

In addition to their thermal effects, astrophysical shocks at velocities $\gtrsim 1000$ km/s always convert at least a few percent of the shock energy into the acceleration of relativistic electrons and ions [13]. In general, this occurs through a first-order Fermi acceleration process. One would thus expect that merger shocks would produce relativistic electrons, which would be observable through radio synchrotron emission. In fact, cluster radio relic and cluster radio halo sources are seen in many clusters (Sec. III). In every case, these clusters appear to be undergoing a cluster merger; the cluster Abell 3667 in Figure (2) is an example. Recent Chandra X-ray images indicate that the radio relics lie just behind merger shocks; the central radio halos may be due to turbulent particle acceleration after the passage of the merger shock [14].

One exciting discovery made with the Chandra X-ray Observatory is the importance of “cold fronts” in merging clusters. Figure (5) shows the cold front seen in the Chandra X-ray image of the central regions of the merging cluster Abell 3667 [15]; this is the same cluster shown in Figure (2). The cold front is the sharp surface brightness discontinuity to the lower right. When these features were first seen, it was initially assumed that they merger shocks, and that the brighter inner region resulted from shock compression. However, X-ray spectral measure-

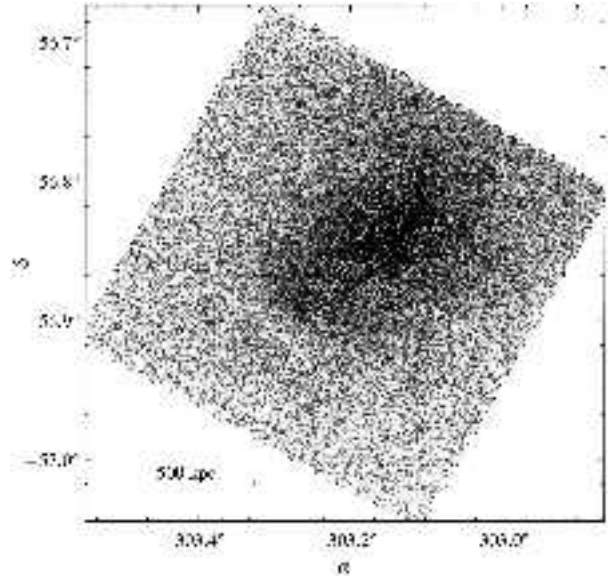


FIG. 5: A “cold front” seen in the Chandra X-ray image of the central region of the merging cluster Abell 3667 [15]. [This is the central region of the same cluster shown in Figure (2).] Note the sharp discontinuity in the X-ray surface brightness. Spectral analysis show that the brighter gas is actually cooler than the surrounding fainter gas. (©2001, The American Astronomical Society.)

ments show that these features are not shocks. The temperature of the denser gas is actually lower than that of the less dense gas in such a way that the pressure is continuous across the surface brightness discontinuity. Thus, the specific entropy is actually lower in the denser region. Shocks are irreversible changes which increase the density, pressure, and entropy. The observed “cold fronts” in clusters are not shocks, but rather contact discontinuities between higher density cool gas and lower density hot gas.

As discussed below (Sec. V), the centers of many clusters often contain relative cool (10^7 K rather than 10^8 K) gas. It is believed that cold fronts occur when clusters containing such cool cores merger. The gas in the core is dense enough to survive for some time after the merger. As the clusters merge, the cool cores move rapidly through the lower density shocked gas, producing the cold fronts.

Observations of cluster merger shocks and cold fronts can be used to derive the kinematics of the merger [15, 16]. Most of these diagnostics give the Mach number of the merger \mathcal{M} , which is the ratio of the merger velocity to the sound speed in the pre-merger gas. The Rankine–Hugoniot jump conditions across a merger shock give the pressure increase across the shock and the shock compression as

$$\frac{P_2}{P_1} = \frac{2\gamma}{\gamma+1} \mathcal{M}^2 - \frac{\gamma-1}{\gamma+1}$$

$$\frac{v_2}{v_1} = \frac{\rho_1}{\rho_2} \equiv \frac{1}{C} = \frac{2}{\gamma+1} \frac{1}{\mathcal{M}^2} + \frac{\gamma-1}{\gamma+1}, \quad (7)$$

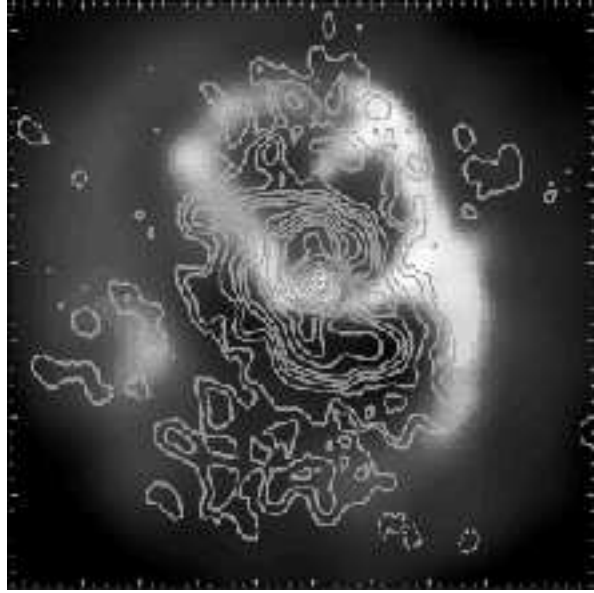


FIG. 6: The grey scale image is the central $\sim 80 \times 80$ kpc of the Chandra X-ray image of the cooling core cluster Abell 2052 [17]. The contours are the radio image of the same region. The hot, X-ray gas is missing from two bubbles to the north (up) and south (down), and bright X-ray shells surround these bubbles. The radio image shows that the bubbles are filled by radio emitting plasma containing relativistic electrons and magnetic fields.

where $\gamma = 5/3$ is the adiabatic index for fully ionized plasma, where $C \equiv \rho_2/\rho_1$ is the shock compression, and the subscripts 1 and 2 denote the pre-shock and post-shock gas. X-ray observations can provide the gas temperature and density on either side of the shock, and the jump conditions yield \mathcal{M} and the merger velocity.

For the case of a cold front, the stagnation condition at the leading edge of the cold front gives [15]

$$\frac{P_{st}}{P_1} = \begin{cases} \left(1 + \frac{\gamma-1}{2}\mathcal{M}^2\right)^{\frac{\gamma}{\gamma-1}}, & \mathcal{M} \leq 1, \\ \mathcal{M}^2 \left(\frac{\gamma+1}{2}\right)^{\frac{\gamma+1}{\gamma-1}} \left(\gamma - \frac{\gamma-1}{2\mathcal{M}^2}\right)^{-\frac{1}{\gamma-1}}, & \mathcal{M} > 1, \end{cases} \quad (8)$$

where P_{st} is the pressure at the stagnation point. If $\mathcal{M} > 1$ there will be a bow shock ahead of the cold front, and one can also apply the shock jump conditions, (Equation 7). The bow shock will be located at some distance (the “stand off” distance d_s) ahead of the cold front, and the ratio of this distance to the radius of curvature of the cold front is a decreasing function of \mathcal{M} . Finally, the opening angle of the Mach cone formed from the merger shock will depend on the Mach number as $\theta_M = \csc^{-1}(\mathcal{M})$.

Applications of these techniques to observed cluster mergers give values for the merger Mach number of $\mathcal{M} \approx 2$ and merger velocities of ≈ 2000 km/s [11, 15].

V. CENTRAL COOLING CORES IN CLUSTERS

At the centers of many clusters of galaxies, the gas temperature is seen to drop significantly from $\sim 10^8$ K further out to $\sim 10^7$ K near the center. At the same time, the gas density rises very rapidly, which gives these regions very large X-ray surface brightnesses. The low gas temperatures and high gas densities are the result of radiative cooling of the gas. Since the X-ray emissivity varies with the square of the density, while the thermal energy density is proportional to the gas density, the X-ray radiation we observe can cool the gas most rapidly in the dense, central regions of clusters. In these regions, the radiative cooling times are $\lesssim 3 \times 10^8$ yr, which is much shorter than the ages of typical clusters of $\sim 10^{10}$ yr. As the central gas cools, the weight of the overlying outer gas compresses the inner gas, resulting in cooler temperatures and very high densities. I will refer to these cool central regions as “cooling cores”.

One mystery with previous X-ray observations was whether the gas continues to cool below $\sim 10^7$ K, and if so, what happens to it. The rates of gas cooling at higher temperature are quite large, and corresponding amounts of much cooling gas are not seen. However, at the center of every cluster with a cooling core, there is a giant cD galaxy. These cD galaxies are the largest galaxies seen in the Universe, and are ~ 10 times larger in mass and radius than other very large galaxies. The cD galaxies at the centers of cooling flows often contain some cool gas and some star formation, although in amounts which are $\lesssim 10\%$ of those expected from the rates of radiative cooling of the X-ray gas.

In nearly every case, these central cD galaxies host radio sources. Recent X-ray observations with the Chandra X-ray Observatory suggest that interactions between the radio source and the X-ray gas in the central regions of clusters strongly affects both components. For example, Figure (6) shows the inner region of the the cluster Abell 2052, which has a cooling core. The central cD galaxy has the strong radio source 3C 317. There are central point sources in X-rays and radio which are coincident with the center of the cD galaxy, which is believed to contain a supermassive black hole. The extended radio emission corresponds with “holes” in the X-ray emission, and the radio source is surrounded by a brightened “shell” of X-ray emission. We refer to these structures as “radio bubbles.” Similar structures are seen in many other cooling core clusters.

The pressures in the X-ray-bright shells are nearly continuous with the pressure of the surrounding gas. There is no clear evidence for strong shocks. Thus, it seems likely that the radio lobes are displacing and compressing the X-ray gas, but are, at the same time, confined by the X-ray gas. The radio bubbles contain relativistic electrons and magnetic fields, and emit radio synchrotron radiation.

The total energy of the the radio plasma is $\sim 10^{59}$ erg. If this energy is eventually dissipated into thermal energy

in the X-ray gas, the energy input would be sufficient to balance cooling for about 10^8 yr, which is about the radiative cooling time of the gas. Thus, energy input from radio sources at the centers of cooling core clusters may partly balance radiative cooling, and may help to explain why only a fraction of the X-ray gas cools to low temperatures.

If there were no physical connection between the radio source and the X-ray emitting plasma in a cluster, then any balance between X-ray cooling and radio source heating would be a coincidence. However, one possibility is that the two are coupled, and form a “feedback loop.” Observations of nearby examples indicate that all large galaxies, such as cluster-central cD galaxies, contain supermassive black holes (SMBHs) with masses of $\sim 10^8 M_\odot$. Radio sources occur when such a SMBH accretes gas from its environment. In radio sources, much of the energy release is converted into the kinetic energy of a pair of oppositely-directed jets of plasma which expand away from the black hole. Consider an inactive SMBH black hole at the center of a cD galaxy in the cooling core of a cluster. If there is no heat source to balance radiative cooling in the X-ray gas, it will cool and flow towards the central supermassive black hole. Part of this gas will be accreted by the supermassive black hole, and the accretion energy (gravitational binding energy) will power radio jets. These will expand into the surrounding X-ray gas, and will inflate two radio bubbles like those in Figure (6). These bubbles will displace and may eventually heat the X-ray gas, balancing its radiative cooling. This will stop the flow of material towards the central SMBH, and eventually turn off the radio source. Heating from the radio source will be unable to prevent cooling of the X-ray gas, and the cycle will start anew. Various arguments suggest that the radio sources in these systems are very strongly active for $\sim 10^7$ yr, and that the cycle

repeats about every $\sim 10^8$ yr.

VI. CONCLUSIONS

Recent observations and theoretical work indicate that the majority of the normal, baryonic matter in the low-redshift Universe is in the form of hot, diffuse plasma. Clusters of galaxies are particularly striking examples of this. Large clusters contain $\sim 10^{14} M_\odot$ of hot plasma at a temperature of $\sim 10^8$ K and typical electron densities of $n_e \sim 10^{-3} \text{ cm}^{-3}$. The total thermal energy content of this plasma is $\sim 3 \times 10^{63}$ erg. This plasma emits most readily in the X-ray band. Recent X-ray observations with the Chandra X-ray Observatory have confirmed that the clusters are formed by the merger of smaller structures, and that merger shocks heat the gas to high temperatures. Mergers may also accelerate relativistic electrons. In the central regions of clusters, the hot plasma cools radiatively. Recent Chandra X-ray Observatory images indicate that the hot thermal plasma interacts with cluster-central radio sources.

Acknowledgments

I am grateful to Huub Rottgering and Alexey Vikhlinin for their very kind permission to use figures from their publications. Support for this work was provided by the National Aeronautics and Space Administration through Chandra Award Numbers GO1-2123X, GO1-2133X, and GO2-3159X, issued by the Chandra X-ray Observatory Center, which is operated by the Smithsonian Astrophysical Observatory for and on behalf of NASA under contract NAS8-39073, and by NASA XMM/Newton Grant NAG5-10075.

[1] G. O. Abell, H. G. Corwin, and R. P. Olowin, *Astrophys. J. Suppl.* **70**, 1 (1989).

[2] N. A. Bahcall, *Phys. Rep.* **333**, 233 (2000).

[3] C. L. Sarazin, *Rev. Mod. Phys.* **58**, 1 (1986).

[4] L. J. Spitzer, *Physics of Fully Ionized Gases* (Interscience, New York, 1956).

[5] T. E. Clarke, P. P. Kronberg, and H. Böhringer, *Astrophys. J.* **547**, L111 (2001).

[6] G. Giovannini and L. Feretti, in *Merging Processes in Galaxy Clusters*, edited by L. Feretti, I. M. Gioia, and G. Giovannini (Kluwer, Dordrecht, 2002), pp. 197–227.

[7] H. J. A. Rottgering, M. H. Wieringa, R. W. Hunstead, and R. D. Ekers, *Mon. Not. R. Astron. Soc.* **290**, 577 (1997).

[8] R. Fusco-Femiano, D. dal Fiume, L. Feretti, G. Giovannini, P. Grandi, G. Matt, S. Molendi, and A. Santangelo, *Astrophys. J.* **513**, L21 (1999).

[9] C. L. Sarazin and R. Lieu, *Astrophys. J.* **494**, L177 (1998).

[10] C. L. Sarazin, in *Merging Processes in Galaxy Clusters*, edited by L. Feretti, I. M. Gioia, and G. Giovannini (Kluwer, Dordrecht, 2002), pp. 1–38.

[11] J. C. Kempner, C. L. Sarazin, and P. M. Ricker, *Astrophys. J.* **579**, 236 (2002).

[12] P. M. Ricker and C. L. Sarazin, *Astrophys. J.* **561**, 621 (2001).

[13] R. Blandford and D. Eichler, *Phys. Rep.* **154**, 1 (1987).

[14] M. Markevitch and A. Vikhlinin, *Astrophys. J.* **563**, 95 (2001).

[15] A. Vikhlinin, M. Markevitch, and S. S. Murray, *Astrophys. J.* **551**, 160 (2001).

[16] M. Markevitch, C. L. Sarazin, and A. Vikhlinin, *Astrophys. J.* **521**, 526 (1999).

[17] E. L. Blanton, C. L. Sarazin, B. R. McNamara, and M. W. Wise, *Astrophys. J.* **558**, L15 (2001).